# Seam-free fabrication of submicrometer copper interconnects by iodine-catalyzed chemical vapor deposition

Sung Gyu Pyo and Sibum Kim
*Hynix Semiconductor Inc., Cheongju, South Korea*

D. Wheeler, T. P. Moffat, and D. Josell[a)]
*Metallurgy Division, National Institute of Standards and Technology, Gaithersburg, Maryland 20899*

(Received 30 May 2002; accepted 1 November 2002)

Kinetic parameters from studies of deposition on planar deposits are used to predict superconformal filling of fine features during iodine-catalyzed chemical vapor deposition. The mechanism behind the superconformal filling is described and the metrology required to predict it is identified and quantified. The dominant effect is the change in coverage of adsorbed catalyst with the surface area during interface evolution. Experimental filling results are described and are shown to be consistent with the predictions. An associated effect on surface roughness of planar deposits is also described.
 [DOI: 10.1063/1.1532931]

## I. INTRODUCTION

Superconformal filling during iodine-catalyzed chemical vapor deposition (CVD) in vias has recently been described.[1–5] It is generally recognized that the likely mechanism for this is the local increase of coverage of adsorbed iodine catalyst at the bottom of the fine features due to a decrease in area during growth.[1–4] In fact, predictions of superconformal filling during surfactant-catalyzed CVD were made by one group.[3] A curvature enhanced accelerator coverage (CEAC) based model, which includes the impact of changing surface area on the local coverage of adsorbed catalyst, was used for the modeling. The kinetics used came from studies of iodine-catalyzed deposition on planar substrates.[6] However, predictions and experiments were not compared because information necessary for a quantitative comparison was not included with the published experimental results.[1,2,4,5] This work describes additional experiments that include all necessary information for quantitative modeling. The results of modeling and experiment are then presented and compared.

## II. EXPERIMENTS

### A. Specimen preparation

Specimens were prepared from planar and lithographically patterned 200 mm silicon substrates. A TiN barrier ≈30 nm thick and a copper seed ≈25 nm thick, both deposited by conventional CVD, were used as the patterned specimens. For catalyzed CVD, iodine was adsorbed on the specimen surface by bubbling carrier gas through $CH_2I_2$ at 80 °C then over the substrates at 150 °C for a specified amount of time. The iodine coverage obtained was determined from total reflection x-ray fluorescence (TXRF) studies with unpatterned specimens. Figure 1 shows the measured dependence of the iodine coverage on the exposure time. Both the iodine adsorption and the copper metal deposits were made in a 200 mm Apex model Cruise-200M reactor (the inclusion of product names is done only for completeness of the description and does not imply NIST endorsement). The copper was deposited using a Cu(I)-hexafluoroacetylacetonate-vinyltrimethylsilane, (hfac)Cu(vtms) precursor (Cupra Select™2504) that was vaporized and introduced into the reactor using a Bronhorst liquid source delivery system with $H_2$ as the carrier gas. The precursor's consumption rate was 0.5 $cm^3$/min unless otherwise indicated.

### B. Studies with planar substrates

Data on the impact of adsorbed iodine on planar deposits is given in Table I and Fig. 2. According to atomic force microscopy, the iodine adsorbed during a 10 s exposure prior to metal deposition decreases the surface roughness significantly (Table I). This effect has been noted previously,[2] including resulting for a $C_2H_5I$ iodine precursor.[5,6] The specimen also becomes more textured based on a decrease of the full width at half maximum of rocking curves around the copper (111) x-ray diffraction peak (Table I). These effects occur along with an increase in the copper deposition rate, which increases monotonically with the coverage of adsorbed iodine (exposure time) as well as the temperature [Fig. 2(a)]. For the conditions used here, transport limited deposition is evident at higher coverage and temperature. The deposition rates were determined from the deposit thickness, obtained by cross-section scanning electron microscopy (SEM) and/or transmission electron microscopy (TEM), and the deposition time.

Quantitative prediction of superconformal feature filling requires the explicit dependence of the metal deposition rate on the iodine coverage. The data at 150 °C are replotted versus the iodine coverage [Fig. 2(b)]; the linear increase of the deposition rate with iodine coverage is consistent with interface kinetics limited deposition. The coverage, obtained using the relationship between exposure time and adsorbed iodine in Fig. 1, is expressed in terms of the fraction $\theta$ of

a)Electronic mail: daniel.josell@nist.gov

 

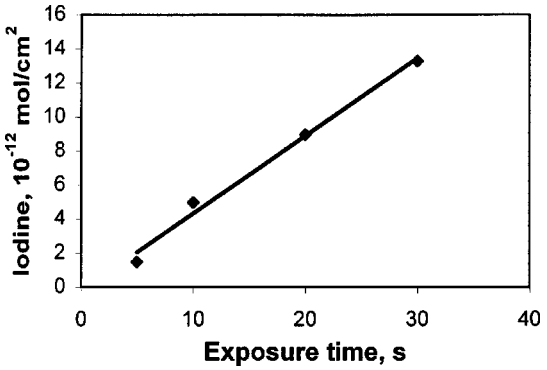


FIG. 1. Dependence of the iodine coverage obtained as a function of the amount of time the planar substrates were exposed to the $CH_2I_2$ precursor vapor (bubbling temperature 80 °C) with substrate temperatures of 150 °C. A linear fit is shown.

estimated saturation coverage $2.9\times10^{-10}$ mol/cm$^2$,[7–9] which is equal to 30% of the total copper sites on a (111) copper surface.

### C. Studies with patterned substrates

For all filling experiments, an initial iodine surface coverage of $\theta_0=0.05$ is anticipated for the 30 s iodine adsorption step used prior to metal deposition. Figure 3 shows the filling sequence of 1 $\mu$m high, aspect ratio 4 (height/diameter) vias at 120 °C. The catalyst adsorbed inside the via has induced filling from bottom to top (superconformal) during copper CVD. Iodine catalyst adsorbed on the field above the via was removed prior to copper deposition using a ''soft'' plasma treatment;[10] the impact on iodine coverage within the features is not known. Figure 4 shows different aspects of superconformal filling of $\approx1$ $\mu$m deep trenches at 150 °C: initially conformal deposition (50 s), the inception of superconformal filling at the bottom corners (150 s), and the overfill bump (420 s). Iodine from the field above the trench was again removed using a plasma. An increase from 150 to 170 °C, coupled with an increase in aspect ratio from 3 to 3.5, results in a shift from superconformal [Fig. 5(a)] to subconformal [Fig. 5(b)] filling of the trenches. The thicker deposits toward the top of the specimen filled at 170 °C are consistent with copper precursor depletion down the trench that arises from transport limited deposition [as per Fig. 2(a)].

TABLE I. Root-mean-square (rms) roughness and peak to valley (maximum height minus minimum height), both obtained using a scanning force microscope over a 5 $\mu$m$\times$5 $\mu$m region near the centers of 200 mm wafers. Similar results were obtained at the edges of the wafers. The FWHM data are from x-ray diffraction rocking curves obtained for the Cu(111) peak. The 10 s iodine exposure time corresponds to iodine coverage of approximately $5\times10^{-12}$ mol/cm$^2$. In each case, copper was deposited for 5 min at the indicated precursor consumption rates with the substrate at 170 °C.

| Iodine pre-exposure, copper precursor flow rate | rms roughness (nm) | Peak to valley (nm) | FWHM (deg) |
|---|---|---|---|
| No iodine, 0.3 cm$^3$/min | 16.3 | 103 | 7.76 |
| 10 s iodine, 0.3 cm$^3$/min | 11.9 | 67 | 7.01 |
| No iodine, 0.5 cm$^3$/min | 14.3 | 103 | 7.54 |
| 10 s iodine, 0.5 cm$^3$/min | 10.0 | 67 | 6.44 |

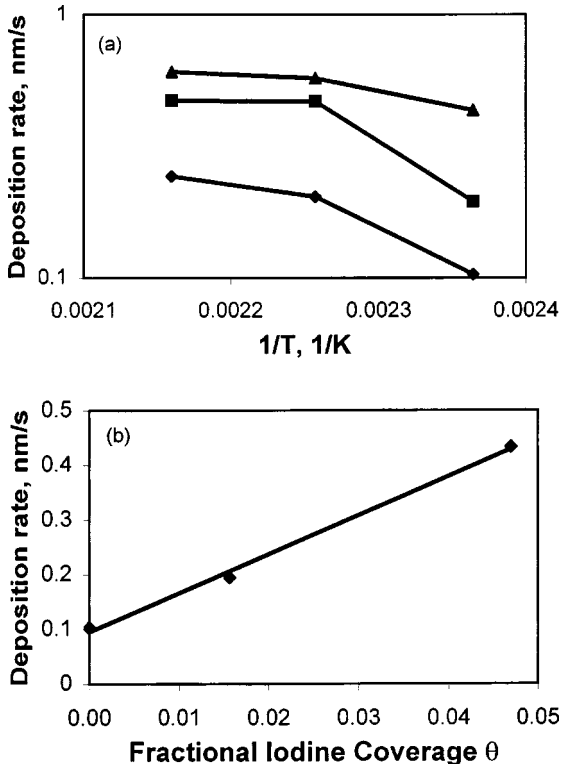


FIG. 2. (a) Dependence of the copper deposition rate (on a log scale) on the temperature as well as on iodine exposure. ◆ 0, ■ 10, and ▲ 30 s iodine exposure). Lines are only intended to guide the eye. (b) The copper deposition rate for substrate temperature of 150 °C increases linearly with the iodine coverage (fit shown).

## III. MODELING FEATURE FILLING

### A. Model

Modeling of the interface evolution is done using CEAC based formalism published in Ref. 3. The dependence of the metal deposition rate, i.e., velocity $v$, on the local coverage of adsorbed iodine $\theta$ is expressed as

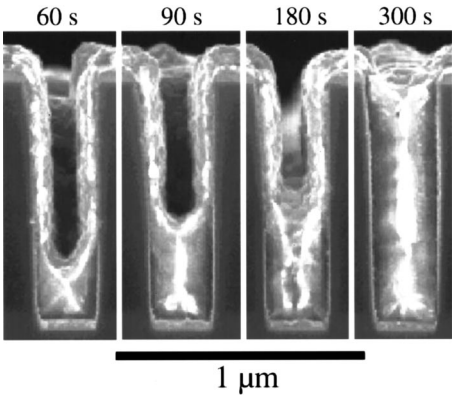


FIG. 3. Filling sequence for 1 $\mu$m high, 0.25 $\mu$m wide vias. The bottom-to-top filling characteristic of the superconformal filling process is evident. Deposition temperature of 120 °C and iodine coverage of $1.3\times10^{-11}$ mol/cm$^2$ (corresponding to $\theta_0\approx0.05$) based on 30 s exposure to $CH_2I_2$ precursor vapor like in Fig. 1. The barrier layer and copper seed layer are 30 and 25 nm thick, respectively.

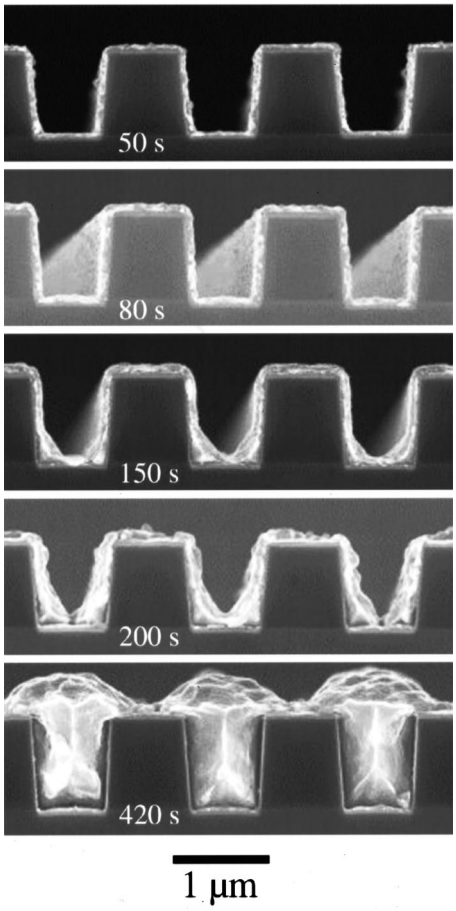


FIG. 4. Trenches 1 $\mu$m high and 0.6 $\mu$m wide after different metal deposition times. Conformal deposition is evident at 50 s. The inception of superconformal filling at the bottom corners is visible at 150 s. Formation of the overfill bump over the superconformally filled features has occurred by 420 s. Deposition temperature of 150 °C and initial iodine coverage of $1.3\times10^{-11}$ mol/cm$^2$ (corresponding to $\theta_0\approx0.05$) based on 30 s exposure to the $CH_2I_2$ precursor vapor like in Fig. 1. The barrier layer and copper seed layer are 30 and 25 nm thick, respectively.

$$v(\theta,T)=(1-\theta)v(0,T)+\theta v(1,T) \tag{1}$$

for $\theta$:[0,1] with the temperature dependent deposition rates on uncatalyzed and fully catalyzed surfaces $v(0,T)$ and $v(1,T)$, respectively. Catalyst coverage beyond $\theta=1$ is presumed to lead to no further increase of the deposition rate. The deposition rate versus iodine coverage relationship at 150 °C

$$v(\theta,150\,^\circ\mathrm{C})\approx0.1+7\theta \ \ (\mathrm{nm/s}), \tag{2}$$

can be extracted from Fig. 2(b). The expression,

$$v_1(\theta,T)=(1-\theta)1.55\times10^7\exp\left(-\frac{7698}{T}\right)+\theta5.6\times10^3\exp\left(-\frac{3007}{T}\right) \ \ (\mathrm{nm/s}), \tag{3}$$

with $T$:(373,573) K, was used in earlier modeling.[3] Equation (3) is based on experimental data from Ref. 6. It predicts deposition rates that are within a factor of 2 of those obtained here. Therefore a modified version of Eq. (2), with a temperature dependence similar to that in Eq. (3), i.e.,

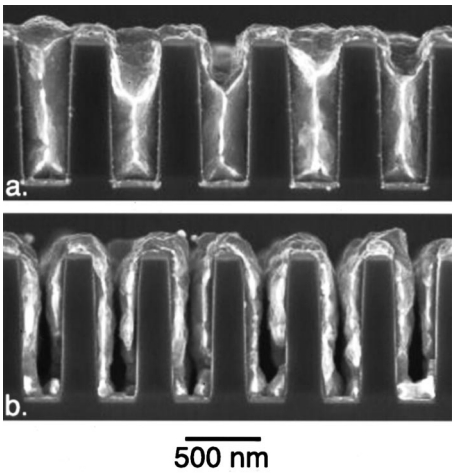


FIG. 5. Experimental dependence of trench filling on the temperature. (a) Filling is superconformal for trenches with aspect ratio of 3 filled at 150 °C. (b) Filling is conformal for trenches with aspect ratio of 3.5 at 170 °C. The trenches are 1 $\mu$m deep. In both cases, the iodine coverage is $1.3\times10^{-11}$ mol/cm$^2$ (corresponding to $\theta_0\approx0.05$) based on 30 s exposure to the $CH_2I_2$ precursor vapor like in Fig. 1.

$$v(\theta,T)=0.1\exp\left[-7698\left(\frac{1}{T}-\frac{1}{423}\right)\right]+\theta7\exp\left[-3007\left(\frac{1}{T}-\frac{1}{423}\right)\right] \ \ (\mathrm{nm/s}), \tag{4}$$

will be used for modeling. Equation (4) converts to the kinetics of Eq. (2) at 150 °C (423 K).

Conservation of the preadsorbed iodine catalyst during copper deposition is ensured locally by

$$\frac{d\theta}{dt}=\kappa v\,\theta, \tag{5}$$

which accounts for the change in coverage caused by the change in area, with the rate of local area change being equal to the local curvature $\kappa$ times the normal velocity $v$. Consumption of the catalyst, e.g., through incorporation into the deposit, is reported to be negligible for iodine-catalyzed copper CVD[1,6] and is therefore ignored here.

A string model was used to track the moving interface and the local catalyst coverage according to Eqs. (4) and (5), respectively.[11] A code that used the sum of both principal curvatures of the three-dimensional (3D) surface was used to model filling of the vias. Depletion of the metal and catalyst precursors within the feature was ignored in the simulations. Failure to fill superconformally in the predictions is indicated by the formation of a seam, characteristic of conformal growth,[11] rather than by a void within the feature.[12]

### B. Simulations of feature filling and comparison to experiment

Iodine coverage on the free surface is presumed to be zero in the model, as intended by the ''soft'' plasma processing, and manifests itself in the minimal deposition on those surfaces in the experiments (Figs. 3 and 4). Figure 6 shows predictions obtained using conditions that correspond to the

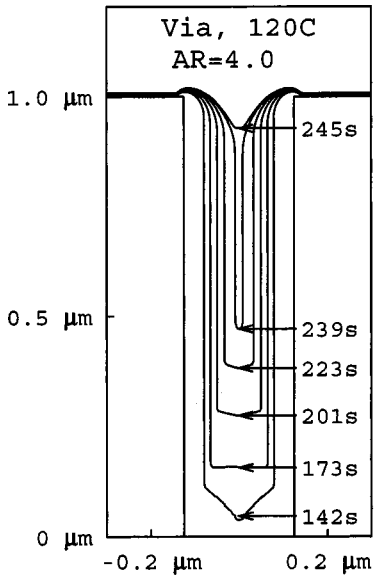


FIG. 6. Predicted fill contours and times for deposition in a 1 $\mu$m high, 250 nm wide via for filling at 120 °C and iodine coverage of $1.3\times10^{-11}$ mol/cm$^2$ (corresponding to $\theta_0=0.05$) for comparison to Fig. 3. The sidewalls are predicted to impinge between 239 and 245 s, and manifesting as a sudden apparent increase in upward velocity of the bottom surface.

via filling experiment in Fig. 3. Consistent with the experimental results, bottom-up deposition is evident for the aspect ratio of 4 via at 120 °C. However, sidewall impingement at between 239 and 245 s prevents its completion. Both the predicted bottom-up filing and the acceleration of the sidewalls are induced by the CEAC mechanism (i.e., a change in local catalyst coverage induced by a change in area). It is unclear whether experiment and predictions match toward the completion of filling, specifically, whether there is a void toward the top of the via (Fig. 3 at 300 s), as predicted by the simulation in Fig. 6.

Figure 7 shows predictions obtained for the trench filling experiment in Fig. 4. Superconformal filling of the 1.3 aspect ratio trench is predicted for the 150 °C deposition temperature, in agreement with the experimental result (although filling takes significantly less time than predicted). The simulations capture the inception of superconformal filling at the bottom corners (150 s) and the overfill bump (420 s). Figure 8 shows simulations of the trench filling experiments in Fig. 5. Consistent with the experimental results, fill is predicted for 150 °C and an aspect ratio of 3 while failure is predicted for 170 °C and an aspect ratio of 3.5. The overfill bump at the far left and the three-quarter filled trench in the middle show the variability in fill times at 150 °C [Fig. 5(a)]. A void that extends farther down the trench than the seam would be

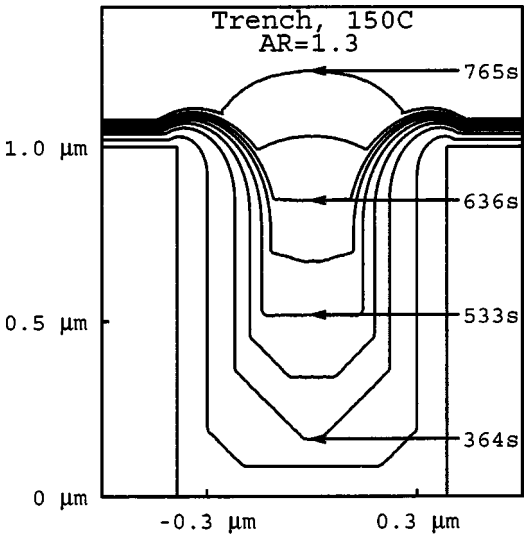


FIG. 7. Predicted fill contours and times for deposition in a 1 $\mu$m high, 600 nm wide trench for filling at 150 °C and iodine coverage of $1.3\times10^{-11}$ mol/cm$^2$ (corresponding to $\theta_0=0.05$) for comparison to Fig. 4.

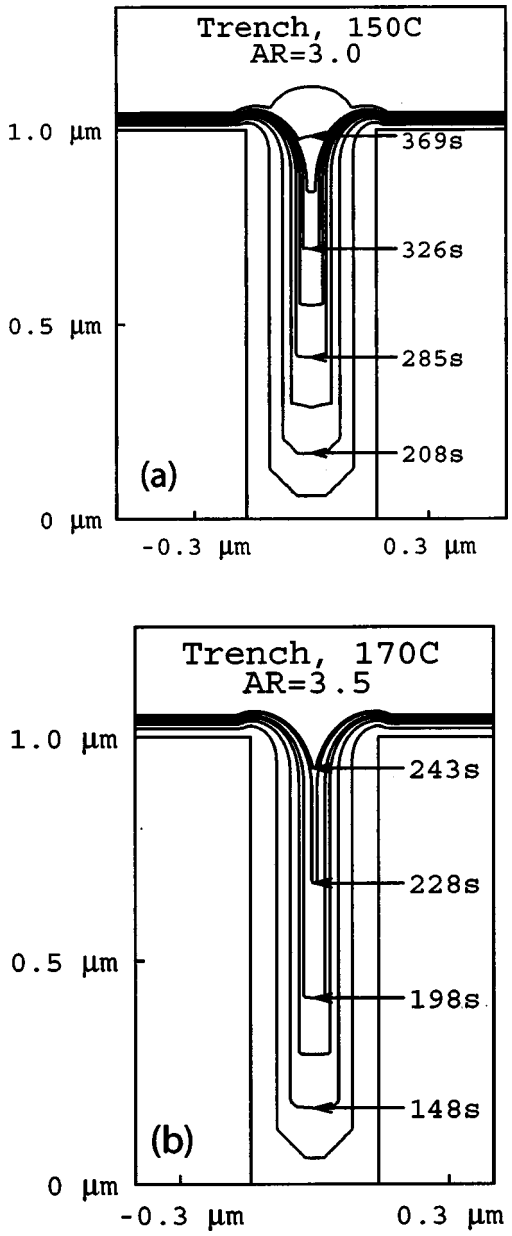


FIG. 8. Predicted fill contours and times for (a) deposition in a trench with aspect ratio 3 filling at 150 °C and (b) deposition in a trench with aspect ratio 3.5 filling at 170 °C. In the second case the sidewalls impinge at ≈235 s, resulting in seam formation in the upper portion of the trench. Both simulations are for 1 $\mu$m high trenches with iodine coverage of $1.3\times10^{-11}$ mol/cm$^2$ (corresponding to $\theta_0=0.05$) for comparison to Fig. 5.

predicted by a code that included depletion[12] for the feature filled at 170 °C.

## IV. CONCLUSIONS

A model based on the curvature enhanced accelerator coverage mechanism was used to describe superconformal filling of fine features during iodine-catalyzed chemical vapor deposition. The CEAC mechanism has previously been used to understand superconformal filling of trenches and vias during the electrodeposition of both copper[11–13] and silver.[14–16]

The CEAC based model successfully predicted whether trenches filled superconformally. Kinetic parameters for modeling were obtained from independent studies of deposition on planar substrates. The CEAC based model accurately predicted the inception of superconformal filling at the bottom corners of the trenches, whether superconformal filling occurred, and the development of a bump over the filled trenches. Fill times were not as accurately predicted.

Superconformal CVD by the CEAC mechanism need not be limited to copper (a conclusion also reached by other authors[4]). This generality has already been demonstrated for electrodeposition with superconformal deposition demonstrated with both copper and silver.[11–16] The only conditions that must be met for superconformal filling by CVD to occur are that (1) the rate limiting step in the CVD processes occurs on the deposit surface (rather than in the vapor) and (2) the adsorbed catalytic surfactant is not consumed (or is consumed very slowly) in the deposition process. For the case of copper CVD from precursor molecules that include hfac ligand(s), it has been suggested that the rate limiting step is the removal and/or desorption of the hfac ligand, possibly through a disproportionation process that coverts two adsorbed Cu(hfac) to one $Cu(hfac)_2$ that volatilizes and a Cu that remains as the metal deposit.[17,18] Based on the results presented here, the presence of the adsorbed iodine accelerates this process; a supposition further supported by experimental results similar to those described here for iodine-catalyzed copper CVD using a different (hfac)Cu based precursor, specifically (hfac)Cu(3,3-dimethyl-1-butene).[19]

[1] H. Park *et al.*, Proceedings of The IEEE 2001 International Technology Conference, 4–6 June 2001, Burlingame, CA, pp. 12–14.
[2] S. G. Pyo, W. S. Min, H. D. Kim, S. Kim, T. K. Lee, S. K. Park, and H. C. Sohn, in *Advanced Metallization Conference (AMC, 2001), Montreal, Canada, October 9–11 2001* (MRS, Warrendale, PA, 2002), pp. 209–214.
[3] D. Josell, D. Wheeler, and T. P. Moffat, Electrochem. Solid-State Lett. **5**, C44 (2002).
[4] K.-C. Shim, H.-B. Lee, O.-K. Kwon, H.-S. Park, W. Koh, and S.-W. Kang, J. Electrochem. Soc. **149**, G109 (2002).
[5] E. S. Hwang and J. Lee, Electrochem. Solid-State Lett. **3**, 138 (2000).
[6] E. S. Hwang and J. Lee, Chem. Mater. **12**, 2076 (2000).
[7] P. H. Citrin, P. Eisenberger, and R. C. Hewitt, Phys. Rev. Lett. **45**, 1948 (1980).
[8] B. Di Cenzo, G. K. Wertheim, and D. N. E. Buchanan, Surf. Sci. **121**, 411 (1982).
[9] B. V. Andryushechkin, R. E. Baranovsky, K. N. Eltsov, and V. Y. Yurov, Surf. Sci. **488**, L541 (2001).
[10] S. G. Pyo, W. S. Min, and S. B. Kim (to be published).
[11] T. P. Moffat, D. Wheeler, W. H. Huber, and D. Josell, Electrochem. Solid-State Lett. **4**, C26 (2001).
[12] D. Josell, D. Wheeler, W. H. Huber, and T. P. Moffat, Phys. Rev. Lett. **87**, 016102 (2001).
[13] D. Josell, D. Wheeler, W. H. Huber, J. E. Bonevich, and T. P. Moffat, J. Electrochem. Soc. **148**, C767 (2001).
[14] T. P. Moffat *et al.*, J. Electrochem. Soc. **149**, C423 (2002).
[15] D. Josell, B. Baker, C. Witt, D. Wheeler, and T. P. Moffat, J. Electrochem. Soc. **149**, C637 (2002).
[16] B. C. Baker, M. Freeman, B. Melnick, D. Wheeler, D. Josell, and T. P. Moffat, J. Electrochem. Soc. (to be published).
[17] G. L. Griffin and A. W. Maverick, in *The Chemistry of Metal CVD*, edited by T. Kodas and M. Hampden-Smith (VCH, New York, 1994), pp. 175–238; see in particular, Secs. 4.3.5 and 4.4, and appropriate references therein.
[18] M. J. Hampden-Smith and T. T. Kodas, in Ref. 17, see in particular, Sec. 5.6.2, and appropriate references therein.
[19] W. H. Lee, B. S. Seo, I. J. Byun, Y. G. Ko, J. Y. Kim, J. G. Lee, and E. G. Lee, J. Korean Phys. Soc. **40**, 107 (2002).